ATMOSPHERIC CHEMISTRY IN THE EARTH SYSTEM: A MODELING APPROACH

GUY BRASSEUR

Free University of Brussels, Belgium
and
National Center for Atmospheric Research, Boulder, Colorado USA

JEAN-FRANÇOIS MÜLLER

Free University of Brussels, Belgium
and
Belgian Institute for Space Aeronomy, Brussels, Belgium

PAUL GINOUX

PIERRE FRIEDLINGSTEIN

Free University of Brussels, Belgium

Abstract

Numerical models are developed to help interpret observations, provide a global representation of complex interactive processes occurring in the earth system, and predict future environmental and climate changes. We describe several models used to study global cycles of chemical species. A two-dimensional model is used to assess potential changes in stratospheric ozone and temperature. A three-dimensional model is used to quantify changes in the chemical composition of the troposphere as a result of human activities. These model studies stress the importance of heterogeneous chemical processes (polar stratospheric clouds, sulfate aerosols) in relation to ozone depletion by chlorofluorocarbons in the lower stratosphere. The relative stability in the oxidizing capacity of the atmosphere since the pre-industrial era is also emphasized. These models should be regarded as components of future earth system models in which global biogeochemical cycles will be simulated. Initial efforts to reproduce the carbon cycle are reported. Future perspectives for chemical-transport modeling are also presented.

1. Introduction

As a result of the agricultural and industrial revolutions, the abundance of several chemical constituents in the atmosphere has been changing rapidly during the 20th century. Some of these gases are radiatively active and, consequently, have reinforced the "greenhouse effect" of the atmosphere. In the case of CO_2, for example, the current trend of 0.4%/yr is a result of fossil fuel burning and, to a lesser extent, of deforestation and changes in land use management. This trend is determined not only by the strength of the anthropogenic emissions, but also by the rates of carbon exchanges between the atmosphere and the ocean, and the atmosphere and the continental biosphere. Large uncertainties in the global carbon cycle need to be elucidated to better quantify the fate of anthropogenic CO_2 (especially under future climate conditions) and the study reported in Section 4 is a partial approach to better understand the exchanges of carbon on the seasonal scale between the atmosphere and terrestrial ecosystems.

The contribution of carbon dioxide in the greenhouse warming over the last 150 years represents only 50% of the total forcing. Methane (CH_4), nitrous oxide (N_2O), and the chlorofluorocarbons (CFC's), whose concentration is currently increasing by 0.6–1%/yr, 0.2–0.3%/yr, and 4–10%/yr, respectively, have also contributed to the warming of the planet. In addition, these gases, which are chemically active, have produced or destroyed other chemical compounds which also interact with solar or terrestrial radiation. For example, the increasing

concentrations of methane and nitrogen oxides have enhanced the chemical production of ozone in the *troposphere*. Ozone, itself a greenhouse gas, has amplified the radiative forcing provided by methane. In addition, the formation of water vapor in the stratosphere, resulting from the oxidation of methane, might have further exacerbated the primary effect of methane. On the other hand, the reduction in the ozone abundance in the lower *stratosphere*, due to the emission in the atmosphere of industrially manufactured chlorofluorocarbons, has probably caused a cooling of the earth's surface. Analyses of satellite data (Figure 1) suggest that, during the 1980's, the column abundance of ozone has decreased by more than 25% over Antarctica in September and October and by as much as 10% at mid-latitudes in the northern hemisphere (e.g., Belgium) from January to April. The ozone depletion has been limited to less than 2% in the tropics.

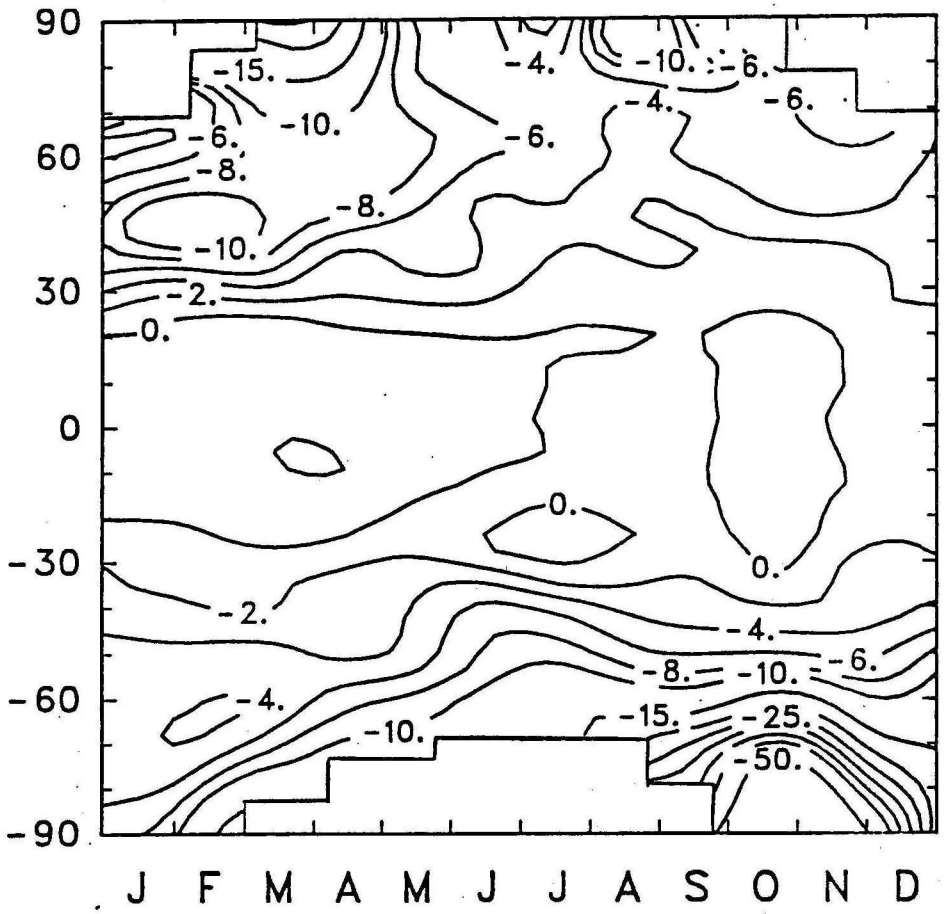

Figure 1. Relative variation (percent) in the ozone column abundance between 1980 and 1990, as a function of latitude and season, deduced from TOMS data.

Preliminary calculations performed with our two-dimensional (2-D) chemical-radiative-dynamical model shows (Figure 2) the change in the radiative forcing as a function of latitude since the pre-industrial era (Hauglustaine et al., 1993). The results stress the potentially important role of chemical feedbacks on climate and suggest that the radiative forcing is enhanced by 30% when these feedbacks are taken into account. On a global basis, the greenhouse effect of tropospheric ozone represents almost 20% of the total radiative perturbation since pre-industrial times. Note that the effect of sulfur compounds has not been included in Figure 2. Anthropogenic sulfur has contributed to the formation of aerosols, which scatter back to space a fraction of the incoming solar energy. This "cooling" effect has probably been localized in industrialized regions (Europe, North America, Southeast Asia).

Numerical models are now commonly used to simulate the spatial and temporal distribution of chemical compounds in the atmosphere and to establish the budgets associated with the global biogeochemical cycles of these compounds. Such models should, in principle, be able to reproduce exchanges of chemical elements between the atmosphere, the ocean and the continental biosphere, and therefore should be similar to the six box model of the global earth system shown in Figure 3.

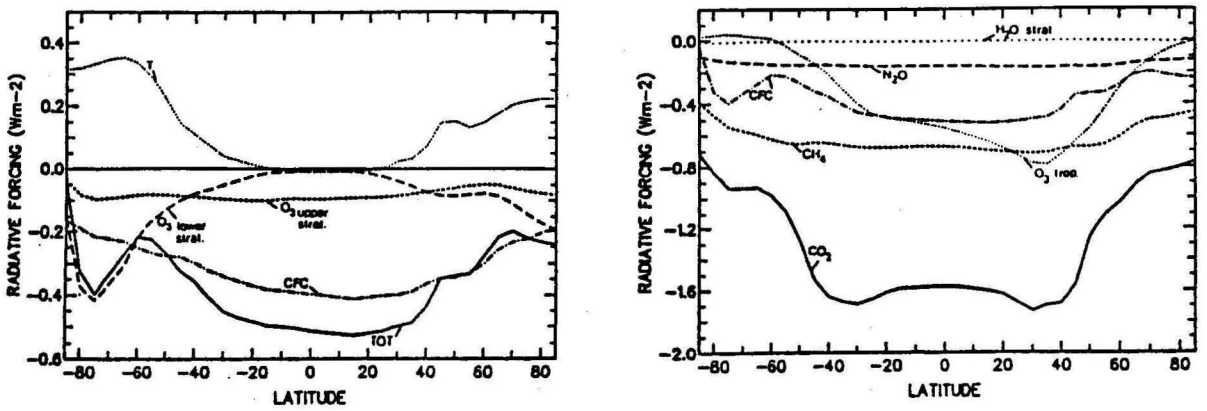

Figure 2. Latitudinal dependence of the calculated radiative forcing due to (a) CFC increase since pre-industrial times (W m^{-2}) and (b) greenhouse gas increase since pre-industrial period (W m^{-2}) (from Hauglustaine et al., 1993).

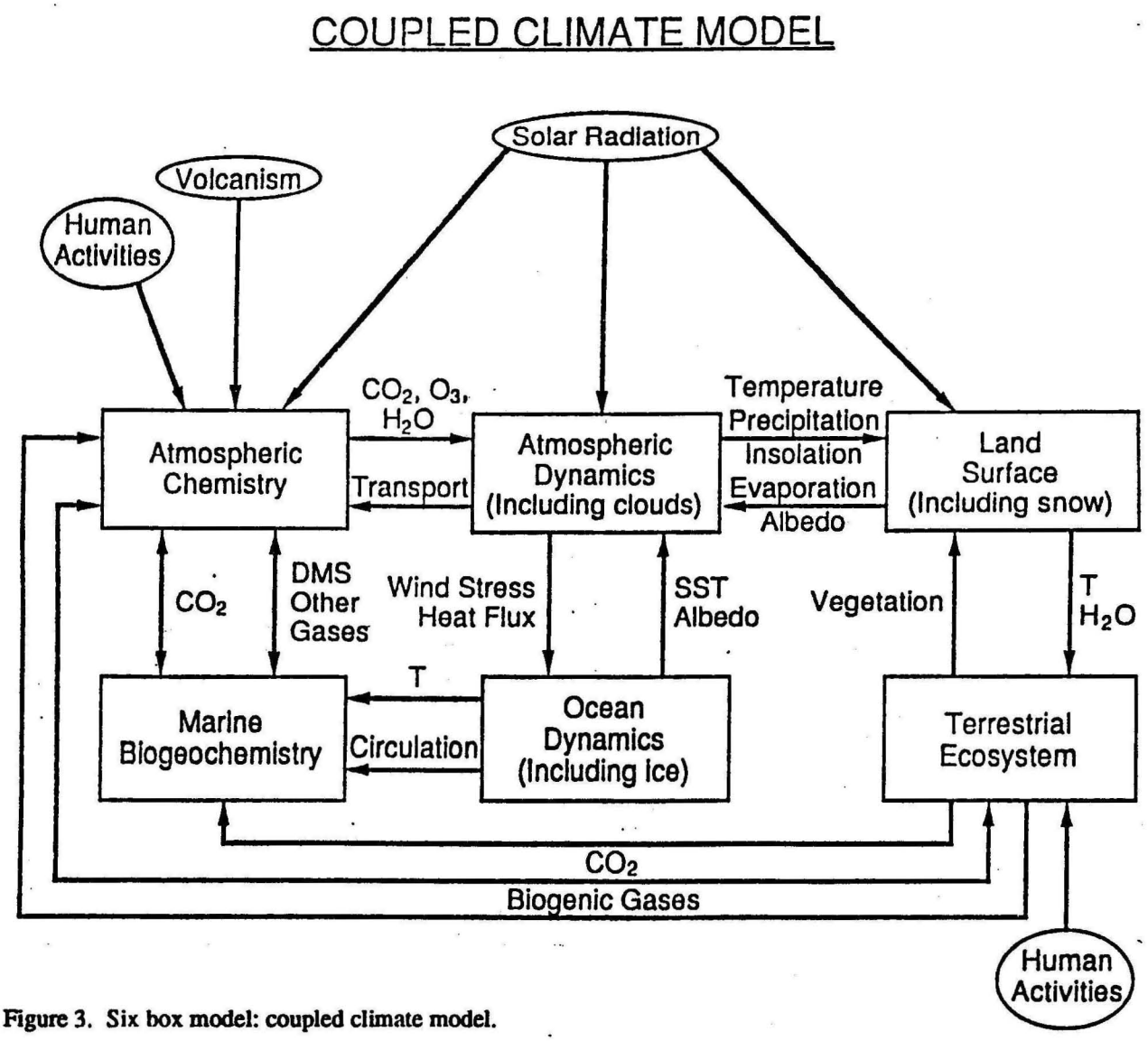

Figure 3. Six box model: coupled climate model.

Although such complex models will be developed in the next decade, and will involve the collaboration of atmospheric chemists, meteorologists, oceanographers, biologists and ecosystem modelers, at this time, a gradual approach needs to be taken. We have therefore developed a hierarchy of models which will be presented in the next sections: (1) A two-

dimensional model which is used to study coupled chemical, radiative and dynamical processes, mostly in the stratosphere; (2) a three-dimensional chemical-transport model (named IMAGES), which is used to simulate the distribution of chemical compounds in the troposphere. With the first of these models, potential changes in stratospheric ozone and temperature as a result of human activities will be established and compared to natural variations (e.g., due to solar activity). With the second model, factors affecting the oxidizing capacity of the atmosphere, and hence the global lifetime of several radiatively active gases, will be determined.

2. The Two-Dimensional Model

The model used to estimate future trends in the ozone abundance is an updated version of the two dimensional model described earlier by Brasseur et al. (1990). It extends from the surface to the mesopause (85 km), with a vertical resolution of 1 km, and from 85°S to 85°N with a latitudinal resolution of 5 degrees. It calculates the 24-hour average of the concentration of 56 species. The concentration of the long-lived species (CO_2, CO, N_2O, HNO_3, N_2O_5, H, H_2, H_2O_2, H_2O, CH_4, HCN, CH_3CN, CCl_4, $CFCl_3$, CF_2Cl_2, CH_3CCl_3, CH_3Cl, CFC-113, CFC-114, CFC-114, CFC-115, CFC-22, Halon 12-11, Halon 13-01, CCl_2O, CClFO, CF_2O, HF, CH_3Br, OCS, SO_2, HSO_3, H_2SO_4) are calculated by solving for each of them a full continuity-transport equation. The short-lived species are grouped into long-lived families (O_x = O_3 + $O(^1D)$ + $O(^3P)$, NO_y = N + NO + NO_2 + NO_3 + HNO_4 + $ClONO_2$ + HNO_3 + 2 N_2O_5, Cl_x = Cl + ClO + HOCl + HCl + $ClONO_2$ + OClO + 2 Cl_2O_2, Br_x = Br + BrO + $BrONO_2$ + HBr + HOBr), for which a full continuity-transport equation is solved. The chemical scheme includes 115 reactions with reaction rates taken from the JPL (1990) compilation (DeMore et al., 1990). Parameterizations of the heterogeneous reactions on particles in polar stratospheric clouds and on sulfate aerosols are included (Granier and Brasseur, 1992). Photolysis and solar heating rates are derived through a spectral integration over up to 171 wavelength intervals. Multiple scattering is taken into account (Luther, personal communication, 1978). The treatment of the infrared (terrestrial) radiation is based on the distributions, calculated by the model, of seven species: CO_2, H_2O, O_3, CH_4, N_2O, $CFCl_3$, CF_2Cl_2 (Briegleb, 1990). The meridional transport of constituents and energy is expressed using the transformed Eulerian mean circulation (Andrews and McIntyre, 1976) driven by momentum deposition associated by gravity wave breaking (Lindzen, 1981) and Rossby wave absorption (parameterization by Hitchman and Brasseur, 1988).

2.1. Model Assessment

Before performing model predictions of future ozone changes, it is appropriate to validate the parameterizations of the heterogeneous chemical processes by simulating the present distribution and past evolution of the ozone.

2.1.1. Ozone Trends

As a result of continuous release in the atmosphere of chlorofluorocarbons (CFCs), and because of the long lifetime (50–100 years) of some of these compounds (e.g., CFC-11 or $CFCl_3$; CFC12 or CF_2Cl_2), the chlorine load (e.g., HCl) of the atmosphere has increased by approximately 4–5% per year (Mankin and Coffey, 1983; Wallace and Livingston, 1991; and Rinsland at al., 1991) over the last decade. Ozone is affected by chlorine through the catalytic cycle:

$$Cl + O_3 \rightarrow ClO + O_2$$
$$ClO + O \rightarrow Cl + O_2$$
$$\overline{O_3 + O \rightarrow 2\,O_2}$$

The model used earlier shows that, when using historical emissions of CFC's and

observed increase in the surface concentrations of carbon dioxide, methane, nitrous oxide as well as other halocarbons, the changes in the ozone column abundance calculated for the 1980–1990 period are small and even slightly positive except at high latitudes in winter. A significant ozone decrease is found in the upper stratosphere and the negative high latitude changes in the ozone column result from downward transport of ozone depleted air masses by the meridional circulation in winter.

The trends in the ozone column derived by the model are significantly different from the observed values derived for the 1980-1990 period by Stolarski et al. (1991) and based on TOMS data.

Specifically, the model with only gas-phase chemistry does not reproduce the formation of an "ozone hole" over Antarctica in September and October nor does it explain the substantial ozone decrease observed at midlatitudes in the northern hemisphere during the winter season. It is now widely accepted, based on laboratory studies and observational evidence, that the sharp decrease in Antarctic ozone is associated with the elevated concentration of inorganic chlorine inside the cold polar vortex where polar stratospheric clouds are observed (WMO, 1989). These clouds are composed of particles which provide surface area needed for heterogeneous reactions. These reactions convert the oxides of nitrogen (e.g. N_2O_5) into nitric acid (HNO_3) and chlorine reservoirs (e.g., HCl, $ClONO_2$) into more reactive forms of chlorine (Cl_2, HOCl, $ClNO_2$). As the Sun returns over Antarctic region, these latter chlorine molecules are photodissociated and, during daytime, the mixing ratio of ClO inside the polar vortex reaches values 50 or 100 times higher than at mid-latitudes. At the same time, especially in the coldest regions where the relatively large ice particles undergo sedimentation, the air masses are progressively denitrified, so that the recombination between ClO and NO_2 is inefficient. Hence active chlorine remains present in large quantities and ozone destruction by catalytic cycles can occur in few weeks.

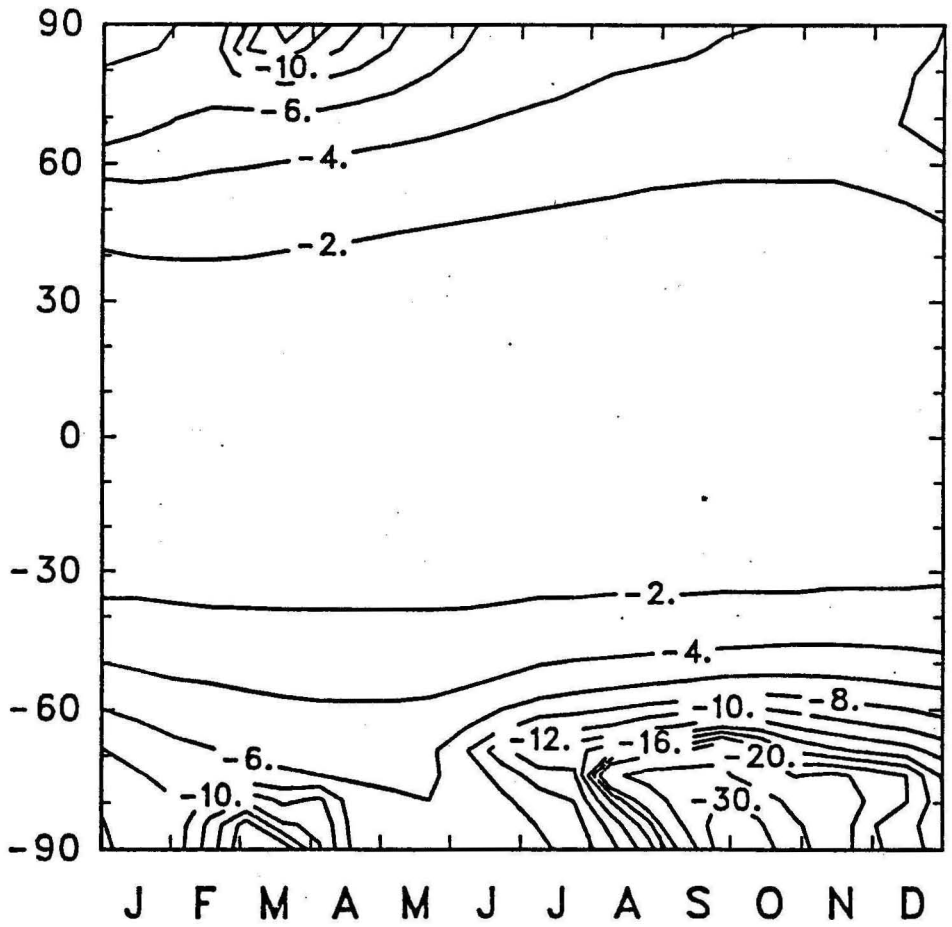

Figure 4. Relative variation (percent) in the ozone column abundance between 1980 and 1990, shown as a function of latitude and season. Heterogeneous chemistry in polar stratospheric clouds and on the surface of sulfate aerosol particles is included in the model calculation.

When these processes are introduced in the model, a substantial ozone decrease is predicted for the 1980–1990 period, especially at high latitudes in the southern hemisphere. The model produces the springtime ozone hole, as the ozone column abundance at 99°S in October is 40% smaller in 1990 than in 1980. Significant but less pronounced ozone reductions are predicted at midlatitudes during all seasons in the southern hemisphere, consistent with the analyzed TOMS data. It can be noticed that no substantial ozone trend is predicted by the model over the Arctic due to a higher temperature and planetary waves activity.

Despite the fact that the chemical effects of polar stratospheric clouds has been introduced in the model, the calculated trend in the ozone column abundance, especially in the northern hemisphere, remains smaller than that derived from satellite monitoring. A possible explanation for the observed ozone destruction at midlatitudes in winter is the impact on stratospheric chemistry of the sulfate aerosol layer. Laboratory investigations (Tolbert et al., 1988; Worsnop et al., 1988) suggest that heterogeneous reactions similar to those occurring in polar stratospheric clouds could operate on the surface of aerosol particles at all latitudes. Figure 4 shows the calculated ozone trend for the 1980–1990 period when the additional chemical effect of sulfate aerosol is taken into account. The trend is closer to the observed values (Figure 1), although quantitative differences still exist. More detailed model calculations and laboratory measurements are clearly needed to better quantify the role of the aerosol layer in past and potential future ozone trends.

The simple but realistic parameterization of the heterogeneous chemistry in our two-dimensional model allows us to reproduce the main features of the past year's observations concerning the ozone distributions with some differences associated with the two-dimensional character of the model formulation.

2.2. Perturbations Studies

Models are used to predict future changes in the chemical composition of the atmosphere and are frequently adopted as the basis for regulatory measures limiting the production of environmentally harmful chemical compounds. We have used our two-dimensional model to assess future changes in the global ozone abundances due to natural and anthropogenic perturbations.

2.2.1. The Solar Cycle Effects

Because the chemical composition of the atmosphere is directly affected by photochemical processes, the effect of solar variability on the abundance of chemical compounds needs to be understood as a prerequisite to assessments of potential anthropogenic perturbations. The solar variability increases with decreasing wavelength and reaches 60–70% at Lyman–α (121.6nm) on different timescales. The most pronounced variability is associated with the 11-year solar cycle. An observed short-term variation in the solar flux results from the uneven distribution of active regions on the Sun which rotates with an apparent period of 27 days. Figure 5 shows the response in the ozone column abundance calculated for a solar variability of 11 years. The change in the ozone column from solar minimum to solar maximum is close to 1% near the equator and increases with latitude, especially in winter. These theoretical estimates are somewhat smaller than the values derived from the analysis of satellite data (Keating et al., 1992). The values are lower than the short-term variability associated with dynamical fluctuations but cannot be neglected compared to the long-term trend in ozone reported for example by Stolarski et al. (1991) for the 1980-1990 period. Thus the effect of solar variability has to be included in the statistical treatment of ozone data, when trying to isolate anthropogenic changes.

2.2.2. The Effect of High Speed Aircraft in the Stratosphere

New plans for the development of a supersonic transport having been produced, and previous studies having shown that release of nitrogen oxides by aircraft engines near 20 km produce an ozone depletion, while emission in the troposphere would lead to an enhancement of

ozone, the two-dimensional model, described earlier, has been used to evaluate the ozone variation due to a fleet of these aircraft.

The emissions scenarios recommended by NASA (Ko, personal communication, 1990; Brasseur, 1992) have been chosen, with an emission of NO_x and other compounds between 16.5 and 20 km altitude in the northern midlatitudes. The calculated reduction in the ozone column abundance (Figure 6) is of the order of 0.7% over the equator and increases towards the north pole. The depletion at high latitudes is largest in summer (4.8% at 90°N), when the catalytic destruction of O_3 is most efficient, while the reformation of ozone by O_2 photolysis is slower than in the tropics.

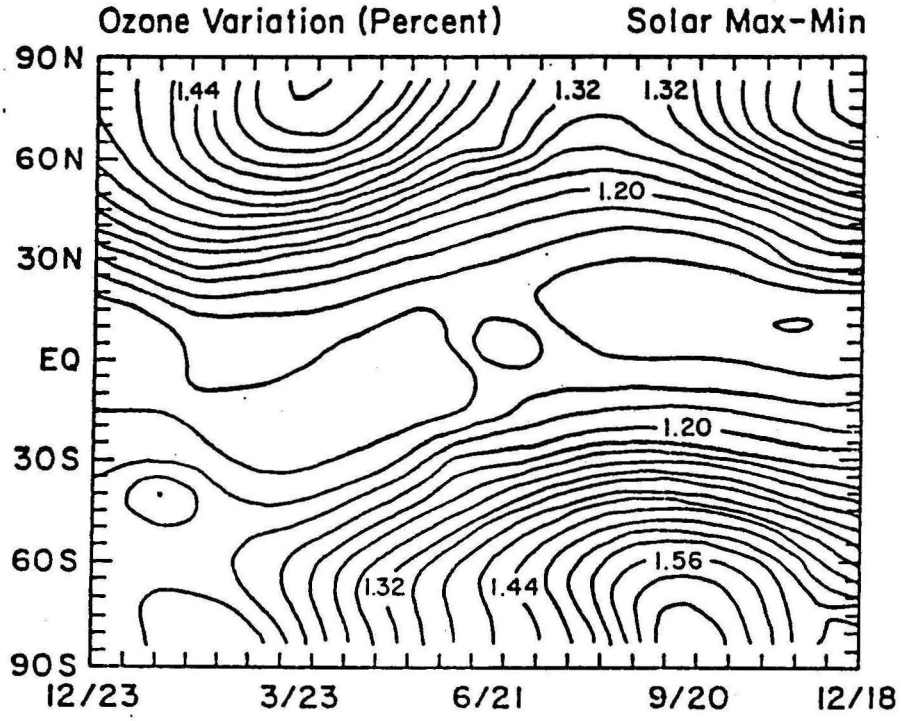

Figure 5. Relative variation (percent) in the ozone column abundance as a function of latitude and time of the year, in response to an increase in solar ultraviolet radiation from solar minimum to solar maximum conditions (11-year solar cycle).

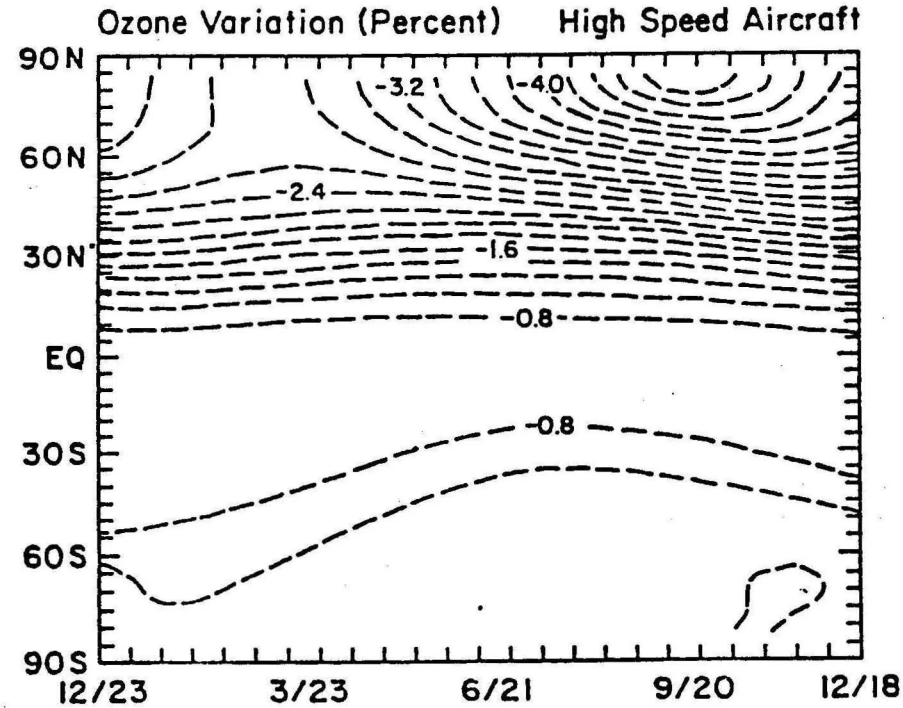

Figure 6. Relative change (percent) in the ozone column abundance calculated at steady state for an injection in the lower stratosphere of nitrogen oxides by a fleet of high altitude aircraft.

Several major uncertainties in this calculation need to be underlined. First, the residence time of the released nitrogen oxides depends on the strength of the stratosphere/troposphere exchanges which are poorly parameterized especially in two-dimensional models. Second, in these calculations, the potential effect of heterogeneous chemistry has been ignored and could reduce significantly the magnitude of the ozone depletion.

2.2.3. The Effects of Chlorofluorocarbons

Halocarbons other than the fully halogenated chlorofluorocarbons have been considered as potential candidates to replace the widely used CFC's, because they contain hydrogen atoms and are partly destroyed by OH in the troposphere. However, the alternative halocarbons absorb infrared radiation, and contribute therefore to the greenhouse effect of the atmosphere. A scenario has been constructed (Brasseur, 1992) to approximately account for expected reductions in the production of halocarbons in relation with the Montreal Protocol (1987) and London Revision (1990). The evolution of the ozone density between 1960 and 2020 for this scenario is shown in Figure 7 as a function of latitude and height for October. A large decrease near 40–50 km altitude is visible (about 8% over the equator and more than 30% at high altitudes). In October, almost all the ozone is destroyed near the South Pole between 15 and 25 km altitude. The ozone increase calculated between 25 and 30 km altitude (and which greatly affects the changes in the ozone column) is a consequence of the "self-heating" effect of the atmosphere and of the cooling associated with the CO_2 increase. The positive change in tropospheric ozone results from the upward trend in the methane concentration. The change in the temperature for the 1960–2020 period is shown in Figure 8. The calculated cooling reaches 13K near the stratopause and is of the order of 3 K at 30 km. The temperature change appears to be relatively uniform with latitude, so that changes in the dynamics of the stratosphere are expected to be relatively small.

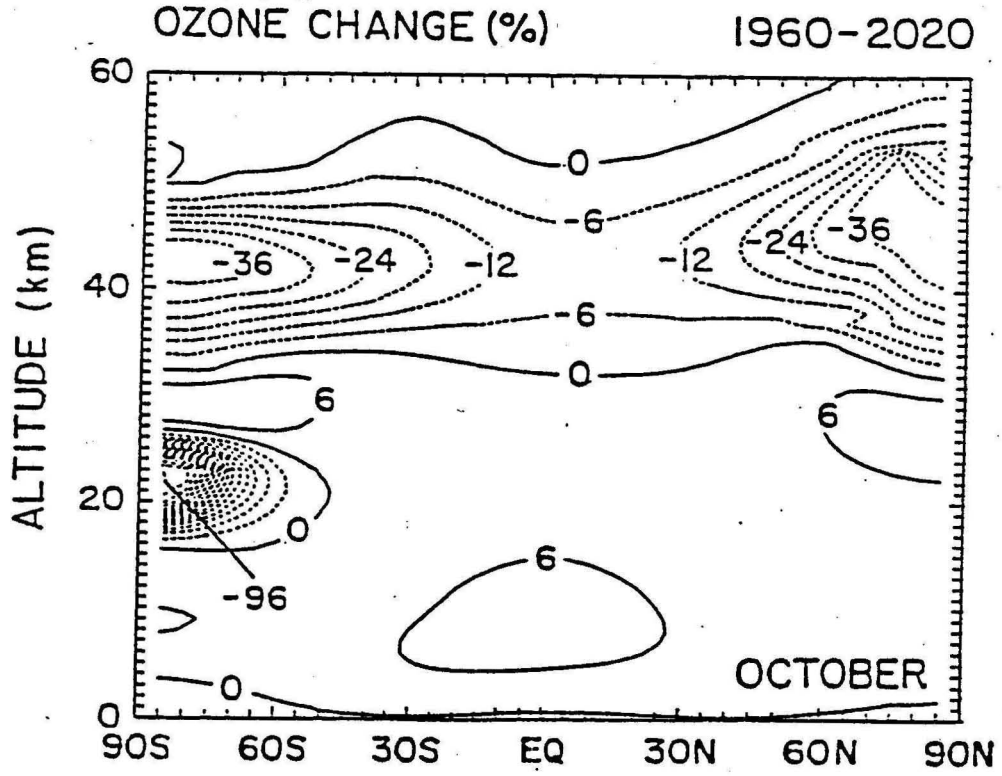

Figure 7. Relative change in the ozone concentration (percent) between 1960 and 2020 represented as a function of latitude and altitude for October.

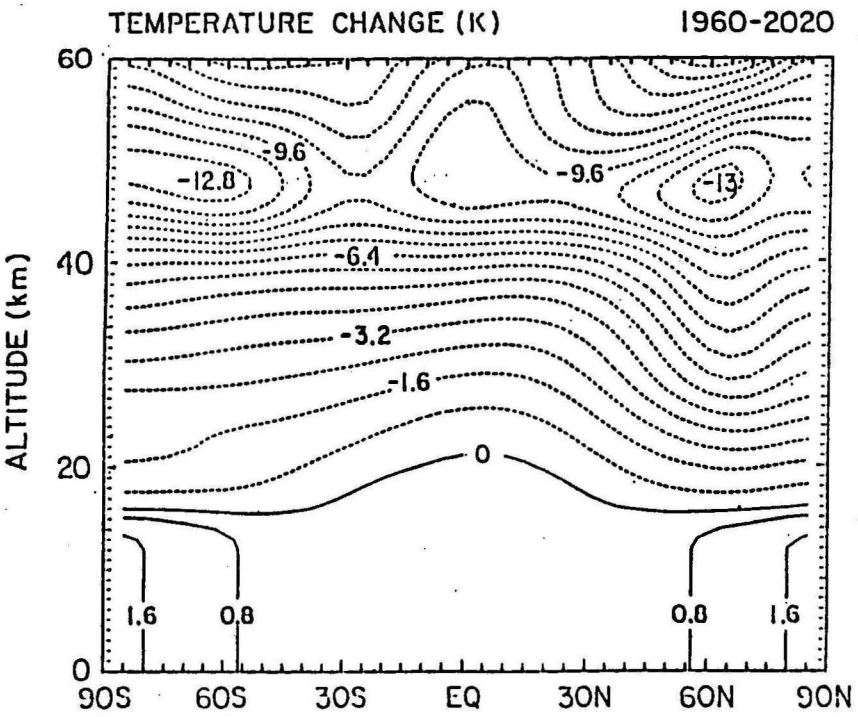

Figure 6. Change in the temperature (Kelvin) between 1960 and 2020 represented as a function of latitude and altitude calculated for March conditions.

3. The IMAGES Model

3.1 Model Description

IMAGES (Intermediate Model of Global Evolution of Species), a global three-dimensional chemical-transport model (CTM) of the troposphere, is used to simulate the behavior of chemical compounds in the troposphere. It extends from the earth's surface to approximately 20 km altitude. Its horizontal resolution is 5° in latitude and in longitude. This model can be regarded as intermediate between models in which the transport is driven by the dynamics provided at each time step by a General Circulation Model, and models in which the transport is highly parameterized, such as in two-dimensional formulations. The chemical scheme is also intermediate between those used in "box models" and in existing 3-D global CTM's. The motivation for such approach is to simulate the three-dimensional behavior and seasonal evolution of a relatively large number of trace constituents, and to estimate their global budgets without prohibitive computer costs. The model provides the distribution of 40 species including ozone (O_3), hydrogen compounds (OH, HO_2, H_2O_2), nitrogen compounds (NO, NO_2, HNO_3,...), CO, several hydrocarbons (CH_4, C_2H_6, C_3H_6, isoprene,...) and oxygenated organic species. The chemical mechanism introduced in IMAGES includes more than 120 reactions, most of them related to nonmethane hydrocarbons chemistry (Müller, 1993). The use of a variable time step (between 1/2 hour and one day) and of a complex diurnal averaging method allows the model to calculate the seasonal variation as well as the diurnal cycle of the concentrations of the chemical species.

The transport of chemical species is driven in the model by monthly mean winds taken to an analysis of the observed winds, from the European Center for Middle Range Weather Forecast (ECMWF) (Trenberth and Olson, 1988a; b). The effects of dynamical variations on time scales smaller than a month are parameterized by eddy diffusivities determined from the observed wind variability (Murgatroyd, 1969; Müller, 1993). The rapid vertical mixing in the planetary boundary layer is also parameterized as diffusion in the continuity equation. The deep convection of trace gases associated with the formation of Cumulonimbus clouds is also represented.

One of the main purpose of the model is to assess the mechanisms that determine the oxidizing capacity of the atmosphere, and in particular, the concentration of the hydroxyl radical (OH). OH is the major sink for many atmospheric trace gases (among them methane) that are emitted at the Earth's surface, as a consequence of human activities. The model is intended to investigate the relationships existing between tropospheric chemistry and climate, for example, through the greenhouse potential of chemically controlled species such as ozone and methane.

3.2 Surface Emissions

The surface emissions and deposition velocities of trace gases used in the model rely on the detailed inventory by Müller (1992). This study assessed the geographical distribution and the seasonal evolution of the emissions associated with technological activities (mainly fossil fuel burning and industry), biomass burning (forest and savanna fires, and also the burning of fuelwood and agricultural wastes), vegetation foliage, the soils, lightning, the oceans, etc. The emissions were estimated using various geographical and economical atlases and statistics. The distribution of the deposition velocities of the most important trace gases were also determined. Deposition velocities are used in models to represent the irreversible absorption of some species by the Earth's surface or by vegetation. The global emissions are summarized in Table 1.

Table 1. Global emissions of trace gases.

Category (Tg/yr). NMHC = nonmethane hydrocarbons	Technological Sources	Biomass Burning	Biogenic Sources (continental)	Oceans	Total
CO	383	784	165	165	1497
NO_2	72	15	22	0	109
CH_4	132	58	270	10	470
NMHC	97	55	498	100	750

To illustrate the results, the geographical distributions of carbon monoxide emissions are displayed in Figure 9. The high emission rate of CO predicted in developed countries are due to the importance of technological sources for this species. Biomass burning explains the highest CO emission rates found in tropical Africa and South America.

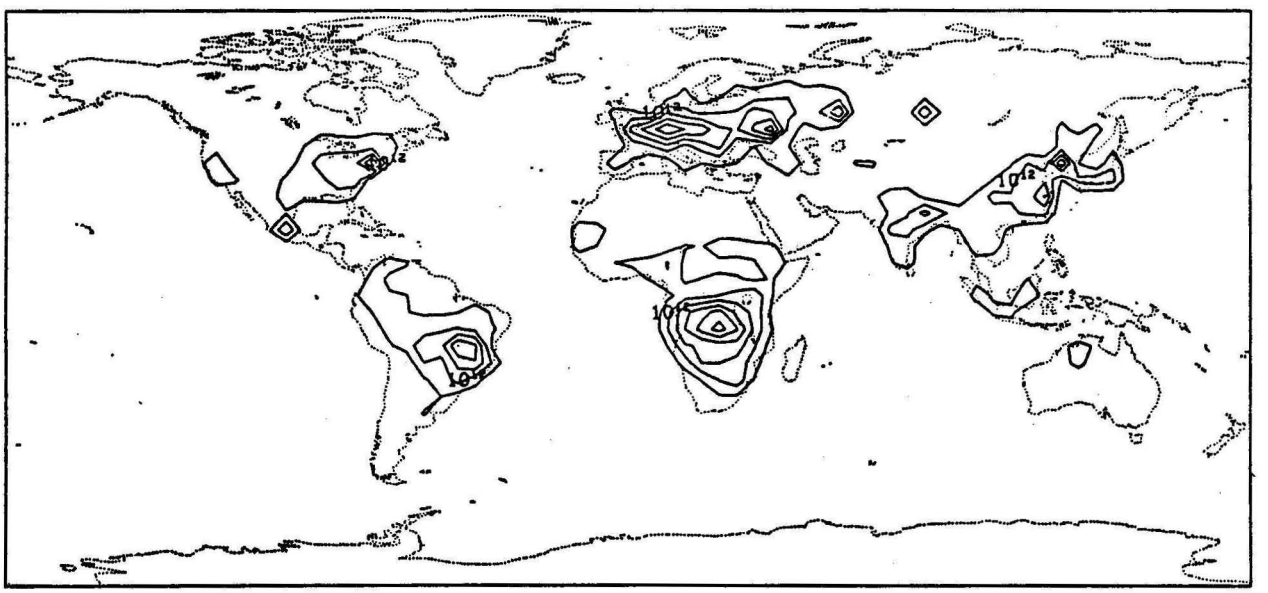

Figure 9. Surface emission of carbon monoxide (CO) used in the IMAGES model for the month of June (molec./cm^2/s). The contours range from 5.10^{11} to 3.10^{12} with a step of 5.10^{11}.

3.3 Model Results for the Present-day Atmosphere

The results provided by the model for the present-day atmosphere agree with the available observations, as far as the large-scale variations of the concentrations are concerned. Since the model uses monthly mean dynamical variables and emissions, however, the small-scale variability of the atmospheric composition is not entirely represented. This does not affect the results of the models regarding the climatological distributions and the budgets of the chemical species calculated by the model. We will now briefly discuss some important results.

Due to their short chemical lifetimes, the nitrogen oxides (NO_x) are predicted to be mostly concentrated in the vicinity of the regions where they are produced. As anthropogenic emissions are the primary contribution to their production, the highest concentrations are found in the boundary layer of the most polluted areas, i.e., over Europe, North America and the Far East (Figure 10a). Due to the role played by nitric oxide (NO) in the photochemistry of tropospheric ozone, important rates of photochemical production of ozone will therefore take place in these regions. The emissions by the soils and by biomass burning explain the secondary maximum of NO_x concentration in continental regions of the tropics. The effect of transport is noticed over the Atlantic and the Western part of the Pacific. In remote areas such as the Central Pacific, NO_x concentration is only of a few parts per trillion (ppt), i.e., about three orders of magnitude less than in polluted areas. Although carbon monoxide (CO) has a much larger chemical lifetime, its distribution close to the surface is still largely determined by its surface emissions (see Figure 10b). The highest mixing ratios of CO are found in Equatorial Africa, where the surface emissions related to biomass burning and the soils add to an important production due to the oxidation of hydrocarbons, notably isoprene. Large mixing ratios are also predicted above developed countries, due to anthropogenic emissions.

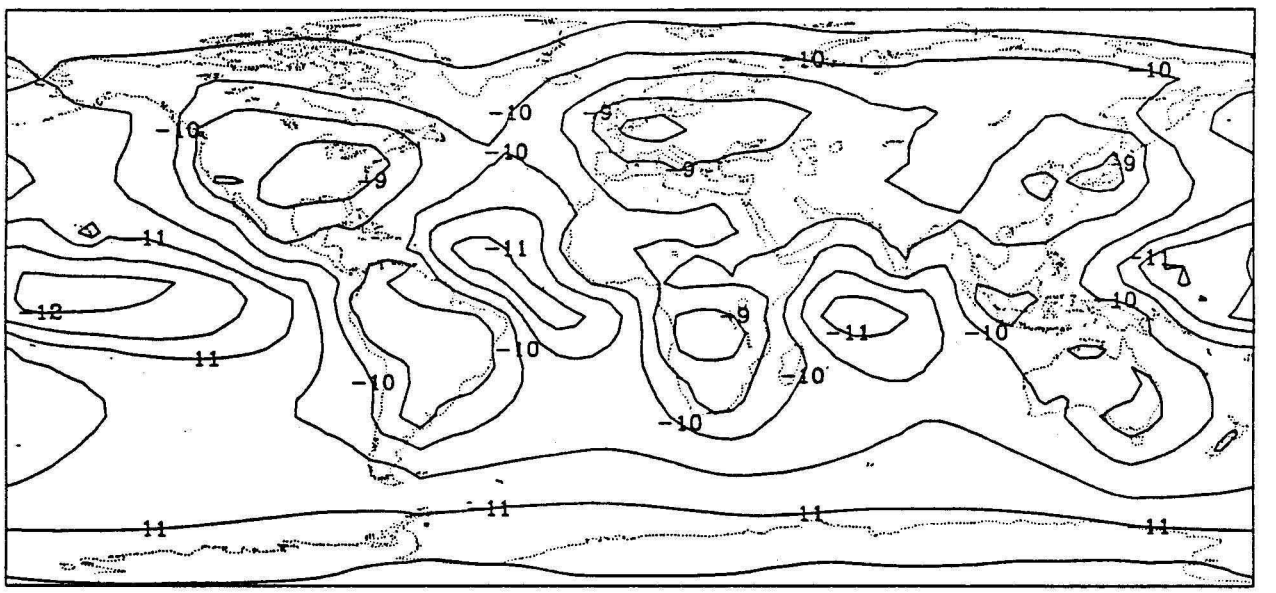

Figure 10a. Mixing ratio of nitrogen oxides (NO_x) predicted by IMAGES (log scale) at 40 meters altitude, in June. Contours range from -12 to -8.5 with a step of 0.5.

Photochemical production of ozone in the troposphere is related to sunlight and the concentrations of nitrogen oxides, carbon monoxide and the hydrocarbons. For this reason, surface ozone concentration is very high during summertime in the northern midlatitudes (Figure 10c). The largest mixing ratios are found over the Mediterranean Sea, due to the vicinity of polluted areas and to the lower deposition velocity of ozone over the ocean, compared with its value over land. Note also from Figure 8c, the secondary ozone maximum in the western part of Central Africa, caused by the emissions related to biomass burning.

Despite its low atmospheric concentration (about 7×10^5 molec./cm^3 on global average), the hydroxyl radical plays a key role in atmospheric chemistry, due to its high reactivity. As

already mentioned, OH is responsible for the largest part of the methane sink. OH is mainly controlled by sunlight, ozone, nitric oxide, carbon monoxide and methane. Its concentration is the largest in tropical regions, in the summer hemisphere. The annually averaged photochemical lifetime of methane predicted by the model is about 10 years, in very good agreement with recent estimates based on considerations about the budget of methylchloroform (Crutzen, 1991; Prinn et al., 1992).

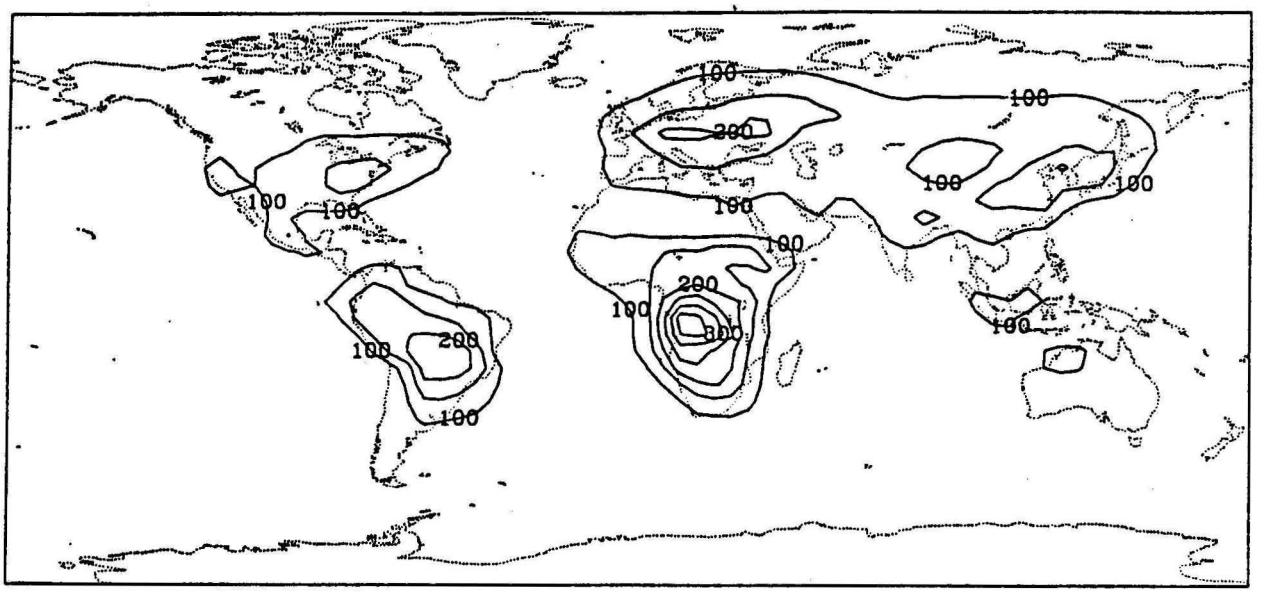

Figure 10b. Mixing ratio of carbon monoxide (CO) predicted by IMAGES at 40 meters altitude in June. Contours range from 100 to 350 with a step of 50.

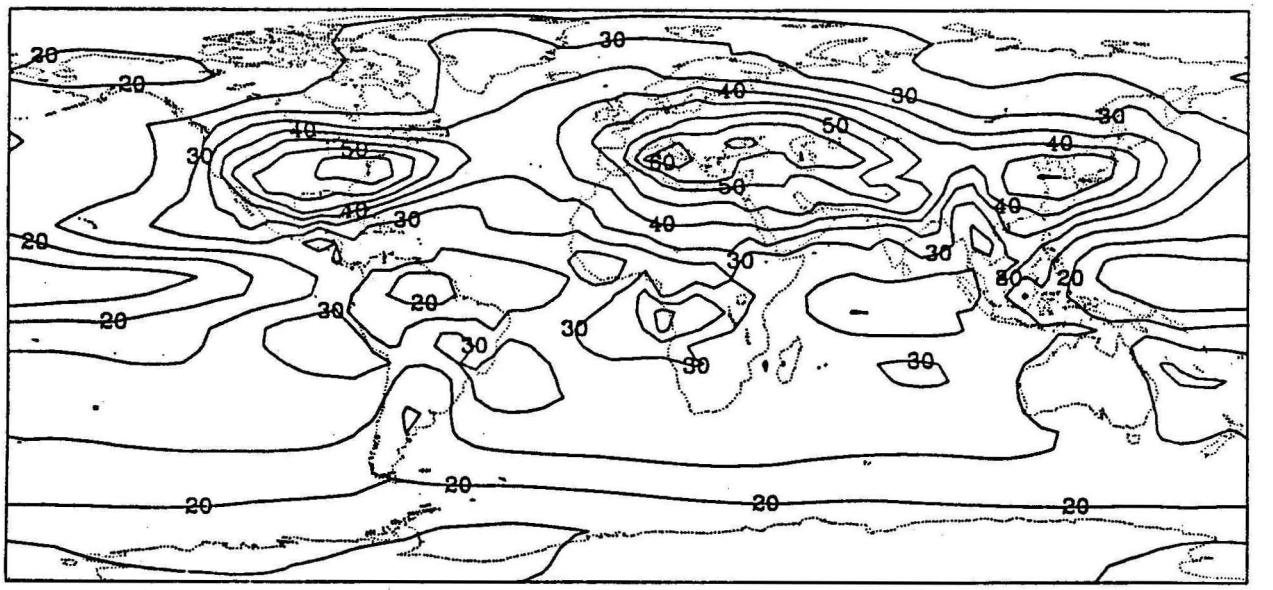

Figure 10c. Mixing ratio of ozone (O_3) predicted by IMAGES at 40 meters altitude in June. Contours range from 15 to 60 with a step of 5.

3.4 The Pre-industrial Atmosphere

The IMAGES model can be used as a tool to determine the sensitivity of the atmospheric chemical composition to e.g. climatic variations or changes in the trace gases emissions. For example, the chemical composition of the troposphere for conditions corresponding to the pre-industrial time (a few centuries from now) was simulated by the model and compared to the present-day composition. The pre-industrial emissions of trace gases are estimated by assuming

zero contributions from technological sources and biomass burning. The other sources and the dynamical fields are assumed to be the same as they are now. Methane concentrations at pre-industrial times are specified from ice core data. The model results show that the mixing ratios of the most important pollutants, such as ozone, carbon monoxide and the nitrogen oxides dramatically increased since the pre-industrial period. For example, Figure 11 displays the difference in percent between the surface mixing ratio of ozone for pre-industrial and present-day conditions. The effect of industrialization is very apparent over Europe, North America and Japan, where the photochemical production (due to the increased emissions of species associated with pollution) caused a 2–3 fold increase in the surface concentration. This result is in good agreement with a recent analysis of experimental data collected at the turn of the last century (e.g., Volz and Kley, 1988). Far from the most polluted areas, the ozone increase is less pronounced but still large (40–150%).

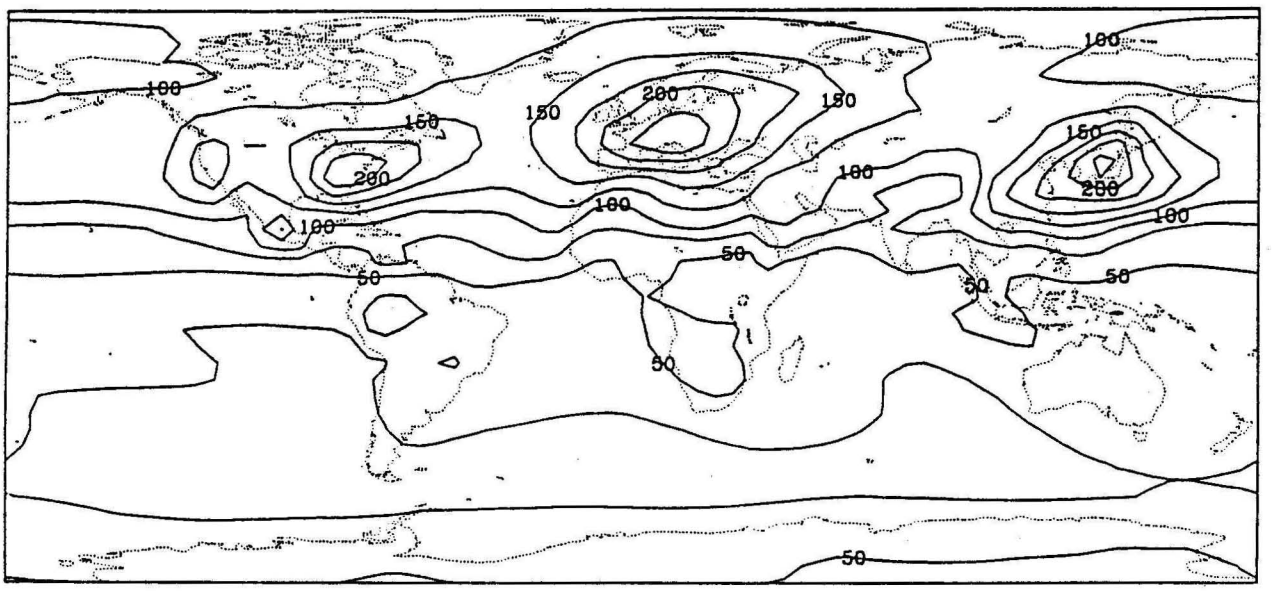

Figure 11. Percentage change in the ozone mixing ratio between pre-industrial and present times (June, 40 meters altitude). Contours range from 25 to 250 with a step of 25.

The oxidizing capacity of the atmosphere is predicted by the model to have only slightly decreased since pre-industrial times. For example, the chemical lifetime of methane increased by about 10%, implying that OH did not change very much on the average. This is an interesting result, as changes in the oxidizing capacity of the atmospheric have long been invoked as a possible cause of the observed increase of the methane concentration. It also means that the mean oxidizing capacity of the atmosphere is not very sensitive to changes in surface-emitted pollutants. The model shows that OH increased by more than 200% over mid-latitudes close to the surface, but decreased in remote areas.

4. Carbon Cycle Model

The global cycle of CO_2 includes fluxes between the atmosphere, the biosphere, and the oceans. An important fraction of the CO_2 released by human activities does not accumulate in the atmosphere, pointing to the existence of large, poorly understood carbon sinks. CO_2 absorption by the oceans was previously believed to be the best candidate for this role (Bolin et al., 1986). However, General Circulation Model (GCM) comparisons with atmospheric CO_2 measurements, and in particular, the observed interhemispheric CO_2 gradient, suggest the existence of a much larger carbon sink in the northern hemisphere than in the southern hemisphere (Tans et al., 1990), suggesting that the continental biosphere be a carbon sink. Reforestation in large areas of temperate and boreal latitudes (Kauppi et al., 1992), and biospheric productivity enhancement due to CO_2 fertilization effect (Bolin et al., 1986) might increase phytomass and therefore store carbon in the terrestrial biosphere. Global biospheric models are then necessary to verify this hypothesis and to assess the quantitative importance of the biosphere in the carbon cycle. Moreover, these models are also needed to help interpret observational atmospheric CO_2 data; the

seasonal variation of atmospheric CO_2 is mainly caused by the seasonal cycle of the biosphere. Any reliable comparison of GCM results with measurements has to involve a realistic model of the biospheric seasonality.

We developed a global, geographically referenced biospheric model. Empirical correlations between the variables describing the continental biosphere and the climate are used, so that the equilibrium response of vegetation to climatic change can be predicted by the model.

The biospheric model predicts the global distribution of nine natural vegetation types and the main carbon pools and fluxes from climatic variables, namely, temperature and precipitation derived from climatology (Shea, 1986). A first version of this model is described in a previous paper (Friedlingstein et al., 1992). Our updated version has several important new features. First of all, the seasonal cycle of the biospheric variables is evaluated, i.e., monthly rather than annual amounts are now calculated. This improvement is fundamental in order to reproduce the atmospheric CO_2 seasonality which is mainly driven by the biospheric activity. Secondly, the relevant carbon flux for studies of atmospheric CO_2 is the net CO_2 exchange between the biosphere and the atmosphere, that is to say, the difference between an atmospheric CO_2 source (heterotropical respiration) and an atmospheric CO_2 sink (Net Primary Production, or NPP). Therefore we include, besides NPP calculation, the computation of the phytomass, litter and soil pools, and their respective production and decomposition fluxes.

We used this model to simulate the Last Glacial Maximum (18,000 years ago) vegetation distribution and its carbon content (Friedlingstein et al., 1992). Results show an important shift from high vegetation types (boreal, temperate and tropical forest) to low vegetation types (tundra, grasslands and deserts) for LGM climate. As a consequence, the phytomass and soil carbon were significantly lower during this glacial period.

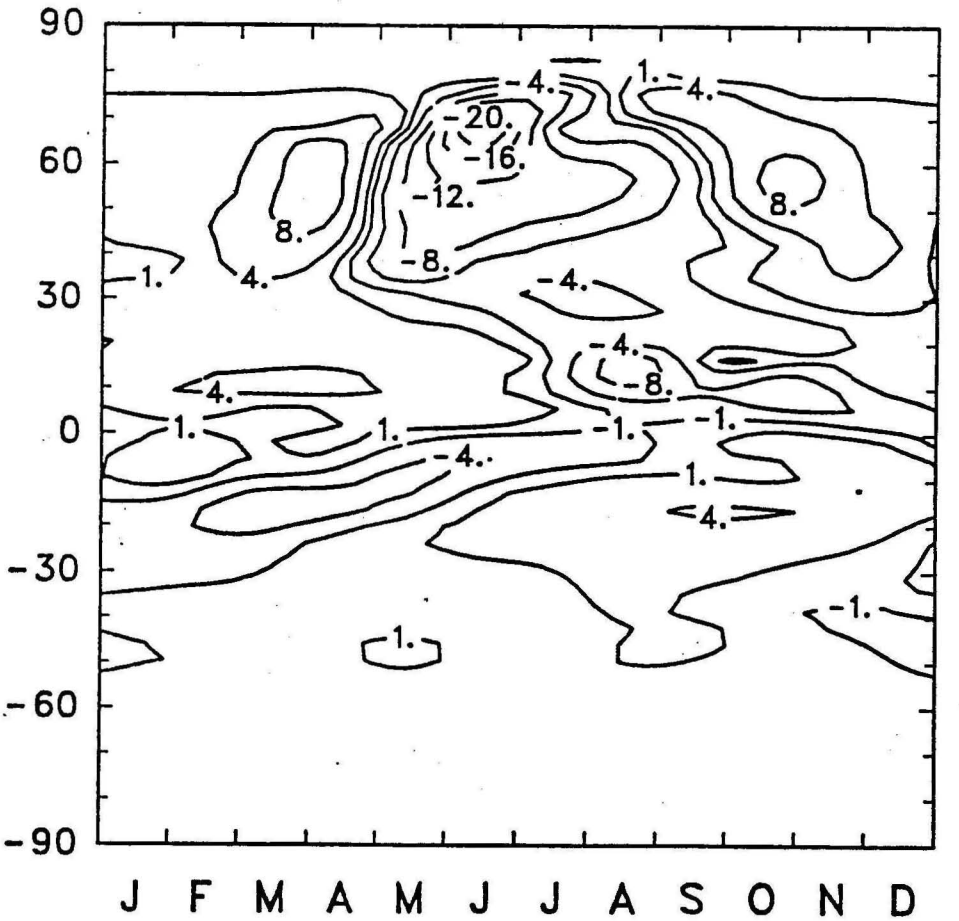

Figure 12. Zonally averaged net CO_2 exchange flux ($gC/m^2/month$) between the biosphere and the atmosphere. Positive values indicate release from the biosphere, negative values correspond to uptake by the biosphere.

For the contemporary carbon cycle, our model reproduces quite well the different pools and fluxes and their seasonal pattern. As an example, the seasonality of the net CO_2 exchange flux (Figure 12) highlights the importance of the northern hemisphere for the atmospheric CO_2 seasonality. In this hemisphere, CO_2 uptake by the biosphere occurs during a relatively short period of time, roughly, from end of spring until end of summer, whereas organic decomposition is occurring from early spring to end of fall and even in winter in temperate and tropical regions. The net flux is then an atmospheric source from September to April and an atmospheric sink from April to September. The southern hemisphere shows a similar pattern but dephased by six months. We compared our model results for the seasonal pattern of the net CO_2 with results from the model of Fung et al. (1987), based on the Normalized Difference Vegetation Index (NDVI). Comparison shows a good qualitative agreement. The carbon fluxes from the latter model has been used in the past to simulate the atmospheric transport of CO_2 (e.g., Tans et al., 1990; Fung et al., 1987). We are presently introducing our biospheric CO_2 fluxes, combined with the other CO_2 sources/sinks (i.e., fossil fuel combustion, deforestation and ocean-atmosphere exchange) into the semi-Lagrangian transport code from the NCAR Community Climate Model (CCM2).

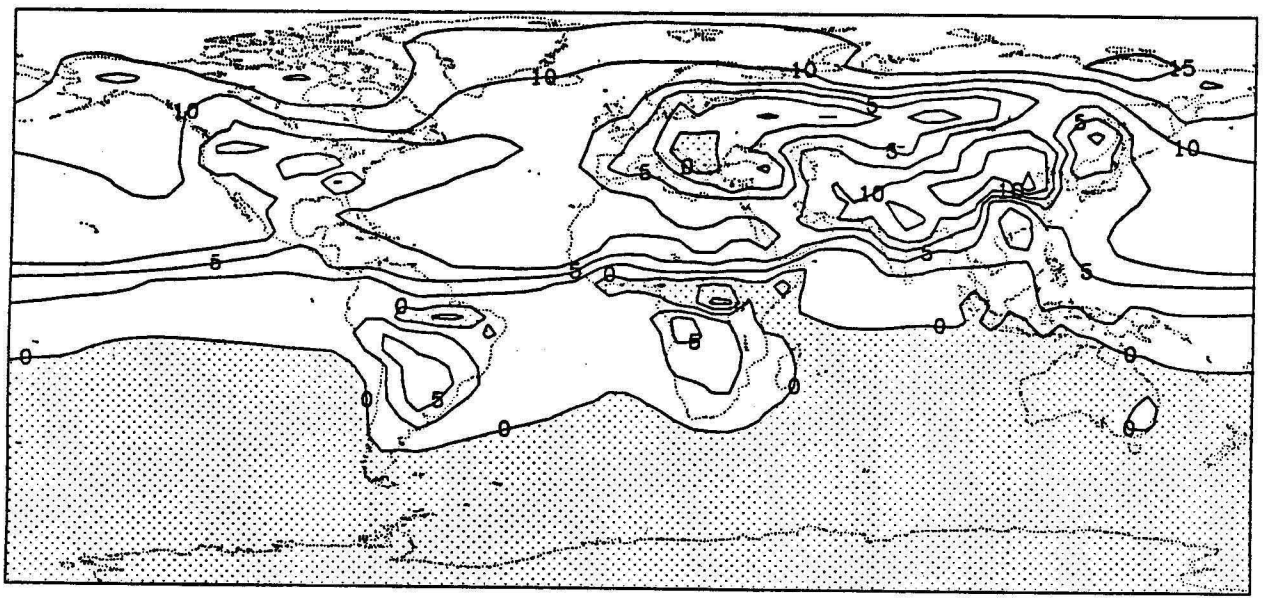

Figure 13.a Mixing ratio of carbon dioxide for july. Add 350 to the values shown to obtain the mixing ratios in ppmv. Contours range from -5 to 15 with a step of 2.5.

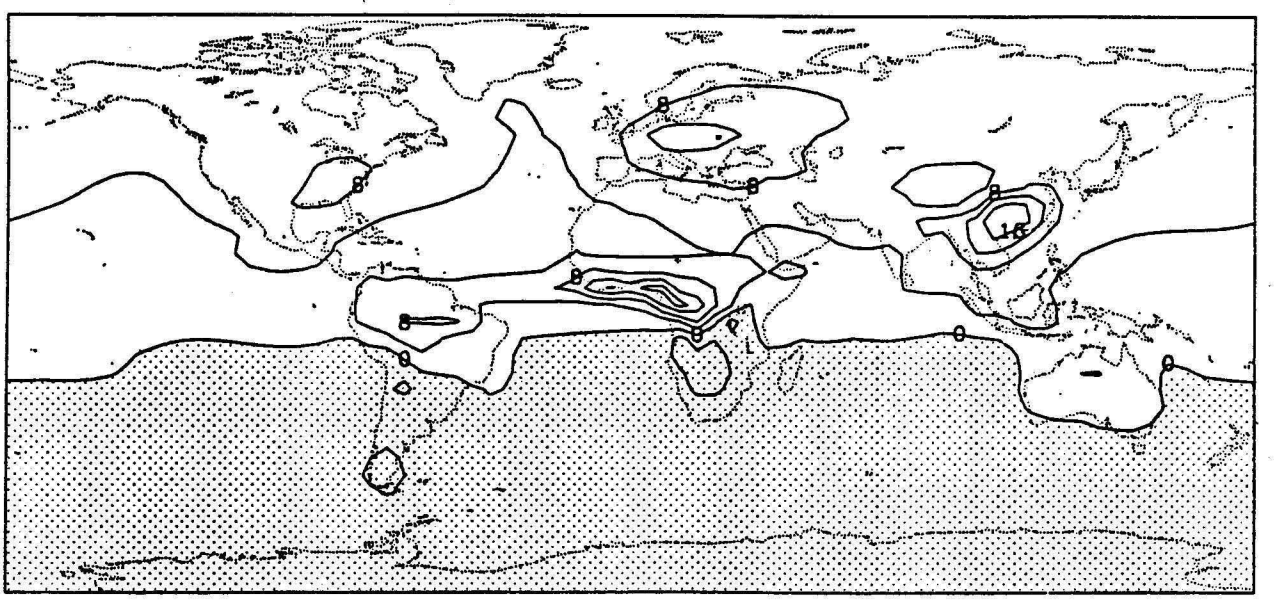

Figure 13.b Mixing ratio of carbon dioxide for December. Add 350 to the values shown to obtain the mixing ratios in ppmv. Contours range from -4 to 16 with a step of 4.

Preliminary tests made with the IMAGES model show (Figures 13a–b) the variation in the mixing ratio of CO_2 in the atmosphere, in relation with the seasonality in the net CO_2 exchange with the continental biosphere. A strong meridional gradient, associated with fossil fuel burning is also visible. Its magnitude is, however, larger than suggested by observations.

5. Future Perspectives for Chemical-transport Modeling

With faster and more powerful computers becoming available, the development of three-dimensional chemical-transport models (CTM's) coupled "on line" with detailed general circulation models (GCM's) will soon become practical. In these models, the distributions of approximately 50 chemical species are calculated and the concentrations of some of them (e.g., ozone) are used to derive radiative properties and dynamical quantities. First attempts have already been completed for the stratosphere by Rasch, Boville and Brasseur (1993). Applications for the troposphere will probably be completed in an "off-line" mode, i.e., the chemistry does not influence the calculated dynamics and temperature. The IMAGES is an attempt to develop such an off-line CTM. A more detailed model forced by the winds provided every 6 hours by a GCM is under development by our group.

Finally, the need for more accurate analyses of available data corresponding to specific meteorological situations has led us to develop a nested model with a spatial resolution increasing towards a region of interest. In such a model, the physical and chemical processes are treated in a climatological sense and with few details on the global (or hemispheric) scale. In the region to be studied in detail, the spatial resolution is higher and meteorological situations (including cloud distributions, precipitation, boundary layer conditions, etc.) are calculated with much detail. To adopt at the same time a global and a regional approach, a complex grid needs to be implemented. Finite elements methods are well adapted to solve numerically the physical and chemical equations involved in the model that is under development.

Acknowledgments. The National Center for Atmospheric Research is sponsored by the National Science Foundation. The authors are grateful to the Service de Programation de la Politique Scientifique and the Institut Belge pour l'Encouragement de la Recherche Scientifique Industrielle et Agricole.

References

Andrews D. G. and McIntyre M. E. 1976. Planetary waves in horizontal and vertical shear: The generalized Eliassen-Palm relation and the mean zonal acceleration. J. Atmos. Sci. 33: 2031–2048.

Bolin, B., Döös B. R., Jäeger J., and Warrick R. A. (eds.). 1986. The greenhouse effect, climatic change, and ecosystems. SCOPE 29. Wiley, Chichester, 541 p.

Brasseur G., Hitchman M. H., Walters S., Dymek M., Falise E. and Pirre M. 1990a. An interactive chemical dynamical radiative two-dimensional model of the middle atmosphere. J. Geophys. Res. 95: 5639–5655.

Brasseur G., Granier C., and Walters S. 1990b. Future changes in stratospheric ozone and the role of heterogeneous chemistry. Nature. 348: 626–628.

Brasseur G., Tallamraju R., Friedlingstein P. and Granier C. 1992a. The impact of high altitude aircraft on the ozone layer, in preparation.

Brasseur G. 1992b. Natural and anthropogenic perturbations of the stratospheric ozone layer. Planet. Space Sci. 40: 403–412.

Brieglieb B. 1992. Long wave band model for thermal radiation in climate studies. J. Geophys. Res. 97: 11475–11485.

Crutzen P. J. 1991. Methane's sinks and sources. Nature. 350: 380–381.

de More W. B., Molina M. J., Sander S. P., Golden D. M., Hampson R. F., Kurylo M. J., Howard C. J. and Ravishankara A. R. 1990. Chemical kinetics and photochemical data for use in stratospheric modeling. JPL Publ. 90-1.

Friedlingstein P., Delire C., Müller J.-F., and Gérard J.-C. 1992. The climate induced variation of the continental biosphere: a model simulation of the last glacial maximum. Geophys. Res. Lett. 19: 897–900.

Fung I. Y., Tucker C. J., and Prentice K. C. 1987. Application of advanced very high resolution radiometer vegetation index to study atmosphere-biosphere exchange of CO_2. J. Geophys. Res. 92: 2999–3015.

Granier C. and Brasseur G. 1992. Impact of heterogeneous chemistry on model predictions of ozone changes. J. Geophys. Res. 97: 18015–18033.

Hauglustaine D. A., Granier C., Brasseur G. P. and Mégie G. 1993. The importance of atmospheric chemistry in the calculation of radiative forcing on the climate system. J. Geophys. Res. submitted.

Hitchman M. H. and Brasseur G. 1988. Rossby wave activity in a two-dimensional model: Closure for wave driving and meridional eddy diffusivity. J. Geophys. Res. 93: 9405–9417.

Kauppi P. E., Mielikäinen K., and Kuusola K. 1992. Biomass and carbon budget of European forest, 1971 to 1990. Science. 256: 70–74.

Keating G. M., Brasseur G., Chiou L. and Hsu C. 1992. Estimating total column ozone response to 11-year solar UV variations using 27-day response as a guide. Submitted to Geophys. Res. Lett.

Lindzen R. S. 1981. Turbulence and stress owing to gravity wave and tidal breakdown. J. Geophys. Res. 86: 9707–9714.

Mankin W. G., Coffey M. T. and Goldman A. 1983. Latitudinal distributions and temporal changes of stratospheric HCl and HF. J. Geophys. Res. 88: 10776–10784.

Müller J.-F. 1992. Geographical distribution and seasonal variation of surface emissions and deposition velocities of atmospheric trace gases. J. Geophys. Res. 97: 3787–3804.

Müller J.-F. 1993. Modélisation tri-dimensionnelle globale de la chimie et du transport des gaz en trace dans la troposphère. Ph.D. Thesis, Belgian Institute for Space Aeronomy, Brussels.

Murgatroyd R. J. 1969. Estimation from geostrophic trajectories of horizontal diffusivity in the mid-latitude troposphere and lower stratosphere. Quart. J. R. Meteorol. Soc. 95: 40–62.

Prinn R., Cunnold D., Simmonds P., Alyea F., Boldi R., Crawford A., Fraser P., Gutzler D., Hartley D., Rosen R., and Rasmussen, R. 1992. Global average concentration and trend for hydroxyl radicals deduced from ALE/GAGE trichloroethane (methylchloroform) data for 1978–1990. J. Geophys. Res. 97: 2445–2461.

Rasch P. J., Boville B., and Brasseur G. P. 1993. In preparation.

Rinsland C. P., Levine J. S., Goldman A., Sze N. D., Ko M. K. W. and Johnson D. W. 1991. Infrared measurements of HF and HCl total column abundances above Kitt Peak, 1977–1990: Seasonal cycles, long-term increases, and comparisons with model calculations. J. Geophys. Res. 96: 15523–15540.

Shea D. J. 1986. Climatological atlas: 1950–1979. NCAR Tech. Note NCAR/TN–269+STR. Natl. Cent. for Atmos. Res. Boulder, Colorado.

Stolarski R. S., Bloomfield P., McPeeters R. D. and Herman J. R. 1991. Total ozone trends deduced from Nimbus 7 TOMS data. Geophys. Res. Lett. 18: 1015–1018.

Tans P. P., Fung I. Y., and Takahashi T. 1990. Observational constraints on the global atmospheric CO_2 budget. Science. 247: 1431–1438.

Tolbert M. A., Rossi M. J. and Golden D. M. 1988. Heterogeneous interactions of chlorine nitrate, hydrogen chloride, and nitric acid with sulfuric acid surfaces at stratospheric temperatures. Geophys. Res. Lett. 15: 847–850.

Trenberth, K. E., and J. G. Olson. 1988a. Intercomparison of NMC and ECMWF global analyses. NCAR Technical Note NCAR/TN-229+STR, Natl. Center for Atmos. Res. Boulder, Colorado.

Trenberth, K. E., and Olson J. G. 1988b. ECMWF Global Analyses 1979–1986: Circulation statistics and data evaluation. NCAR Technical Note NCAR/TN-300+STR, Natl. Center for Atmos. Res. Boulder, Colorado.

Volz A. and Kley D. 1988. Evaluation of the Montsouris series of ozone measurements made in the nineteenth century. Nature. 332: 240–242.

Wallace L. and Livingstone W. 1991 Spectroscopic observations of atmospheric trace gases over Kitt Peak, 3. Long-term trends of hydrogen chloride and hydrogen fluoride from 1978 to 1990. J. Geophys. Res. 96: 15513–15521.

Worsnop D. M., Zahniser M., Kolb C., Watson L., van Doren J., Jayne J., Davidovits P. 1988. Mass accommodation coefficient measurements for HNO_3 on water, ice and aqueous sulfuric acid droplet surfaces. Proceedings of the Polar Ozone Workshop, (extended Abstracts), Snowmass, Colorado, USA.